



RESEARCH

Molecular Characterization of Alfalfa Mosaic Virus and Its Effect on Basil (*Ocimum basilicum*) Tissues in Egypt

Ahmed K. El-Attar¹, Samah A. Mokbel¹ and Om-Hashem M. EL-Banna²

ABSTRACT

Background: Various isolates of *Alfalfa Mosaic Virus* (AMV) found throughout the world affect a wide variety of aromatic and medical plants. In March 2016, several symptoms of leaf necrosis, bright yellow mosaic and malformation of leaves suggested viral infection of AMV on basil plants grown in Beni Suef governorate.

Objectives: The present study aimed to characterize the virus at the molecular level and described the ultrastructural changes or other histopathological alterations in basil cells following infection by AMV.

Methods: Studies were conducted to elucidate the etiology of the disease. The diagnostic tools used were the transmission electron microscope for rapid diagnosis, host reactions, serological double-antibody sandwich (DAS)-ELISA, reverse transcription (RT)-PCR and nucleotide sequence determination. Ultra-structural responses of basil leaf cells infected with a morphologically distinct RNA virus, AMV, were studied. Molecular characterization and phylogenetic analysis were performed for the AMV coat protein (CP) gene. An amplicon of the predicted size (~666 bp) derived from *O. basilicum* isolate was purified and cloned in *E.Coli* into pCR[®]4-TOPO vector before proceeding to DNA sequencing and the alignment of sequences.

Results: Electron microscope examination of negatively stained preparations from symptomatic basil leaves revealed viral particles have a bacilliform structure with particles size of 112.5 nm in length and 57.5 nm in width. Initial microscopic analysis suggested that the described symptoms are caused by AMV. The major effects on cells infected with AMV included disappearance of nucleolus, disruption of nuclear membranes, vacuolated cytoplasm, plasmodesmal dilation, abnormality of chloroplast shape, disorganization of the palisade mesophyll cells and necrosis in the zone of vascular cells. On the basis of mechanical transmission, symptoms induced were similar to those caused by AMV. Presence of AMV in basil plant was further confirmed by the results obtained from the laboratory-based techniques such as (DAS)-ELISA, and RT-PCR using a pair of primers specific to the AMV-CP gene. Phylogenetic analysis results indicated that AMV-Egypt that isolated from Basil is most closely related (96.4%) to the AMV-Spain strain isolated from Hibiscus plants.

Conclusion: Pathological investigation may provide insights into the alterations of the cell after viral infection and understanding of the data concerning the behavior of the virus. Phylogenetic analysis revealed highest identity with the Hibiscus isolate of the AMV that help in the molecular epidemiology of the virus. Particular attention should be given to the possibility of continuous monitoring of isolates of AMV at the molecular level to implement appropriate control measures.

Keywords: Basil; *Alfalfa mosaic virus*; RT-PCR; Cloning; Nucleotide Sequence Analysis; Histopathology; Cell Pathology.

BACKGROUND

Basil (*Ocimum basilicum* L.) of the family (*Lamiaceae*) is one of the oldest known herbal plants in the world. In Egypt, the local cultivated area, reached to 7329 feddan produced 153811tons with an average of 20.987 tons/faddan, most of them concentrated in Giza, Beni Suef, El-Fayoum, El-Monofia and Assiut governorates. In terms of the global trade, Egypt ranked as the fourth (41,664 MT) among the top 23 basil exporters in the world during the 2013 season (FAO/WHO, 2017).

Many different viruses can naturally infect basil plants and responsible for a great deal of damage to leaves. For example, *Alfalfa mosaic virus* (Shafie *et al.*, 1997), *Tomato spotted wilt virus* (Holcomb *et al.*, 1999), *Broad bean wilt virus* (Sanz *et al.*, 2001), *Pepino mosaic virus* (Davino *et al.*, 2009), *Impatiens necrotic spot virus* (Poojari and Naidu, 2013), *Chili leaf curl virus*, *Tomato leaf curl Al Batinah virus*, *Tomato yellow leaf curl virus* (Ammara *et al.*, 2015) and *Cucumber mosaic virus* (Sinha and Samad, 2019).

Among these viruses *Alfalfa mosaic virus* (AMV) is considered as one of the most prevalent plant viruses and the only member of the genus *Alfamovirus* within the family *Bromoviridae*, infects large number of herbs and native plants naturally in over 70 families, which induce a variety of characteristic symptoms on diseased host plants, including bright yellow calico mosaic and chlorotic lesions. It is primarily transmitted via seed, aphids, specifically green peach aphid (*Myzus persicae*), and can also be spread by direct transfer of sap from the infected hosts to the healthy plants (Shafie *et al.*, 1997; Wintermantel and Natwick, 2012).

Alfalfa mosaic virus is a multipartite virus, and is composed of the non-infective three linear RNAs (RNA1, RNA2 and RNA3) and a subgenomic RNA4. The four viral RNAs are separately encapsidated into bacilliform particles. RNA1 and RNA2 contain single open reading frame (ORF) encoding the viral replicas subunits (P1 and P2, respectively). RNA3 contains two ORFs encoding the movement protein and coat protein (CP). The CP is expressed from a fourth subgenomic RNA. The presence of RNA4 or its translation product of AMV-CP plays a major role in the RNA replication, the encapsidation of viral RNA, the interacting with the insect vector and the establishment of systemic infection (Balasubramaniam *et al.*, 2014).

The spreading of AMV in the world has highlighted both the importance of rapid and accurate diagnosis of this disease. Consequently, the need for rapid diagnostic tools as microscopy technique will be increasingly important for detecting infection and/or disease before having to perform the enzyme-linked immunosorbent assay and nucleic acid amplification techniques that required using an expensive range of antisera and/or primers to characterize one of many possible viruses. Indeed, the beam of microscopy covers a wide area of the test specimens and does not require specific reagents but at least lights the way for recognize the pathogenic agents (Otulak *et al.*, 2014; Kumlachew, 2015).

Alfalfa mosaic virus was first reported in basil plants in Egypt by Shafie *et al.* (1997). AMV has been identified on the basis of particle morphology and host reaction as well as traditional serological indexing. Since this report, there has been no published data concerning the sequence of AMV-CP gene or reports on potential adverse effects by AMV on basil tissues in Egypt. The purpose of the present study is therefore to characterize the virus by tests at the molecular level and describe the ultrastructural changes or other histopathological alterations in basil cells following infection by AMV.

MATERIALS AND METHODS

The diagnostic studies of the pathogen were done at Virus and Phytoplasma Research Department, Plant Pathology Research Institute, Agricultural Research Center whereas, samples screening based on microscopy was done at Electron Microscopy lab, Faculty of Agriculture Research Park (FARP), Faculty of Agriculture, Cairo University.

Plant materials source and diagnostic electron microscopy

Samples of diseased basil leaf (both young and old leaves) were collected during early March 2016 after severe mosaic symptoms had been observed on basil plants grown in Beni Suef governorate. The collected leaves with suspicious symptoms of viral infection were washed thoroughly in sterile tap water. The microscopic examinations of the specimens were performed for a preliminary evaluation of the disease situation and the virus or viruses present in the samples using negative staining method according to Noordam (1973). A 5 µl drop of sample to be examined was deposited onto 400 mesh copper grids coated with a thin layer of carbon. A small drop (5 µl) of neutral 2% PTA stain (Phosphotungstic acid, buffered to pH 7 using sodium hydroxide) was then applied to the grid and left for 2 minutes. The excess fluid was blotted by means of a piece of filter paper. The virus particles were examined using the JEOL transmission electron microscope (JEM-1400 TE Japan) at the instrumental magnification of 120000x, and images were captured using CCD camera Model, Optronics camera with 1632x1632 pixel format as side mount configuration.

Serological detection by enzyme-linked immunosorbent assay (ELISA)

Both healthy and symptomatic leaves of basil plants were tested for AMV and some other viruses using double-antibody sandwich (DAS)-ELISA as previously described by Clark and Adams (1977). ELISA kits were supplied by LOEWE Biochemica GmbH (Germany). Other viruses which were tested included *Cucumber mosaic virus* (CMV) and *Tomato spotted wilt virus* (TSWV) using two specific antisera were supplied by Agdia (USA) and Bioreba (Switzerland), respectively. Plant tissue samples were ground in extraction buffer (1:5 w/v). After incubation with p-nitrophenyl phosphate (pNPP, Sigma- Aldrich) at room temperature for 60 minutes in the dark, absorbance at 405 nm was measured with an ELISA microplate reader (Dynatech MR 7000) and samples were considered positive if the absorbance value was higher than twice the absorbance of the negative control. Commercial positive and negative controls were included in each DAS-ELISA test.

Biological purification and host range study

On the basis of the microscopic examination and DAS-ELISA results, AMV was biologically purified by inoculating the extracted crude sap from leaves microscopically positive to leaves of *Chenopodium amaranticolor* according to Kahn and Monroe (1963). The produced local lesions on *C. amaranticolor* were re-inoculated on healthy *C. quinoa* for three consecutive times. The local lesions obtained from the third re-inoculated *C. quinoa* were propagated in *Nicotiana tabacum* var white burley.

In host range studies, induced symptoms-associated with AMV were determined by mechanically inoculating the group of host plants representing four families: *Chenopodiaceae*, *Fabaceae*, *Lamiaceae* and *Solanaceous* (Table 1). Inoculations were conducted by grinding inoculated tobacco leaves in a mortar using 0.01 M phosphate buffer, (pH 7.0) and were performed with the aid of Celite (Sigma-Aldrich) as an abrasive. Under greenhouse conditions, three seedlings of each host plant were inoculated and observed daily for symptom development. The same number of healthy seedlings of the same species and age were left without inoculation to serve as a control. The presence of AMV in host plants was further confirmed by reverse transcription (RT)-PCR assay.

RNA isolation and Reverse transcription (RT)-PCR assay

Total RNAs were extracted from leaves of naturally infected basil and artificially inoculated plants of *N. tabacum* and *O. basilicum* as well as healthy leaf

samples of basil using QIAamp RNA isolation kit (Qiagen, Germany) according to manufacturer's manual. RT-PCR was performed according to standard procedures (Ausubel *et al.*, 1989), using the Verso™ 1-Step RT-PCR Kit (Thermo Fisher Scientific, Waltham, MA, USA) with forward primer AMV-F2 and reverse primer AMV-R2m specific for the coat protein (CP) gene of AMV. The primer set was designed according to Xu and Nie (2006) as the following sequences, the AMV-F2 sequence (5'-ATCATGAGTTCTTCACAAAAGAA-3') and the AMV-R2m sequence (5'-ATGACGATCAAGATCGTCAGC-3'). The reverse primer was modified by deletion of the stop codon and designed to amplify the entire CP gene of AMV when used with AMV-F2. The RT-PCR reaction was optimized to be performed in a final volume of 50 µl. The final concentrations of the reaction components were: 25 µl of 1-Step PCR Master Mix, 200 nM of each forward and reverse primer, 1 µl Verso enzyme mix, 2.5 µl RT-Enhancer and 3 ng of template (RNA). Samples were then processed, after incubation at 94°C for 5 minutes, followed by 35 cycles of 30 sec. at 95°C, 30 sec. at 58°C and 30 sec. at 72°C and an additional extension step at 72°C for 10 minutes in a programmable thermal controller (Biometra, T Gradient Thermocycler, Germany). Amplified products were analyzed by 1% agarose gel electrophoresis, stained with gel star (Lonza, USA) and visualized under a UV transilluminator using Gel Documentation System (Gel Doc 2000, Bio-Rad, USA). A 100 bp DNA ladder (Invitrogen, CA, USA) was used.

DNA sequencing and phylogenetic analysis

PCR-products were purified using a QIAquick PCR purification kit (Qiagen, Canada) and then the purified amplicon, obtained from *O. basilicum*, was cloned into pCR®4-TOPO cloning vector in DH5α *E-Coli* competent cells according to the manufacturer's instructions (Invitrogen, CA, USA) and directly sequenced in both directions using the same primer pair used in RT-PCR. Sequence of the identified AMV isolate in this study was compared with available AMV sequences in GenBank using the BLAST program. The phylogenetic tree was analyzed and constructed using the DNAMAN software, version 4.13; Lynnon BioSoft.

Nucleotide sequence accession number

Sequence data of AMV-CP gene has been submitted to GenBank and assigned accession number MH625710.

Histopathological and ultrastructural studies

Light and transmission electron microscopy were performed using the tissues of both healthy and diseased fresh materials. Depending on size and shape, fresh leaves were cut into small pieces (approx 2mm x 2 mm) in a petri dish containing 2% glutaraldehyde in 0.1 M Na-cacodylate buffer (pH 7.2). Rinsing procedure took place in 0.1 M solution of 0.1 M Na-cacodylate buffer for 45 minutes, with buffer changes at 15 and 30 minutes. The samples were placed in a secondary fixative buffer containing 1% osmium tetroxide (OsO₄) dissolved in 0.1 M Na-cacodylate buffer for 1.5 hours. Following secondary fixation, the specimens were dehydrated in the ethanol-acetone series and imbedded in Spurr's medium according to the method described by (Rocchetta *et al.*, 2007) and adopted by El-Banna *et al.* (2014). Embedded specimens were mounted on blocks. For light microscopy (LM) semi thin sections (1mm) were cut with glass knife and stained with Toluidine blue for five minutes and then mounted in water on glass slides. Slides were examined by OPTIKA B-350 light microscope and photographs were captured using AIPTEK-HD-DV 1080P. For transmission electron microscopy (TEM), the same blocks were thin sectioned (90-100 nm) with diamond knife ultramicrotome (Leica model EM-UC6) and then transferred onto 400-mesh copper grids. Grids were stained with 2% uranyl

acetate and lead citrate (for 10 and 5 minutes, respectively) prior to examination using the JEOL electron microscope (JEM-1400 TE Japan) at the candidate magnification. Photographs were captured using CCD camera model AMT, Optronics camera with 1632x1632 pixel format as side mount configuration.

RESULTS

Symptoms and identification of *Alfalfa mosaic virus*

Naturally infected basil plants exhibited severe symptoms included leaf necrosis, malformation of leaves; folding of leaves towards the main veins with patches of various shades of yellow or white like aucuba, chlorotic leaves (Fig. 1A and B) and bright yellow mosaic on emerging shoots and mature leaves, gave rise to typical calico symptoms (Fig. 1C) as compared to those of healthy ones (Fig. 1D). Negative staining and electron microscopy of tested specimens from symptomatic basil plants demonstrated typical bacilliform particles with 112.5 nm length and 57.5 nm width resembling AMV (Fig. 2). Results of DAS-ELISA indicated that tested basil leaves were free of CMV and TSWV or mixed infections while, only positive results were obtained when the collected infected samples were tested using the AMV antiserum.

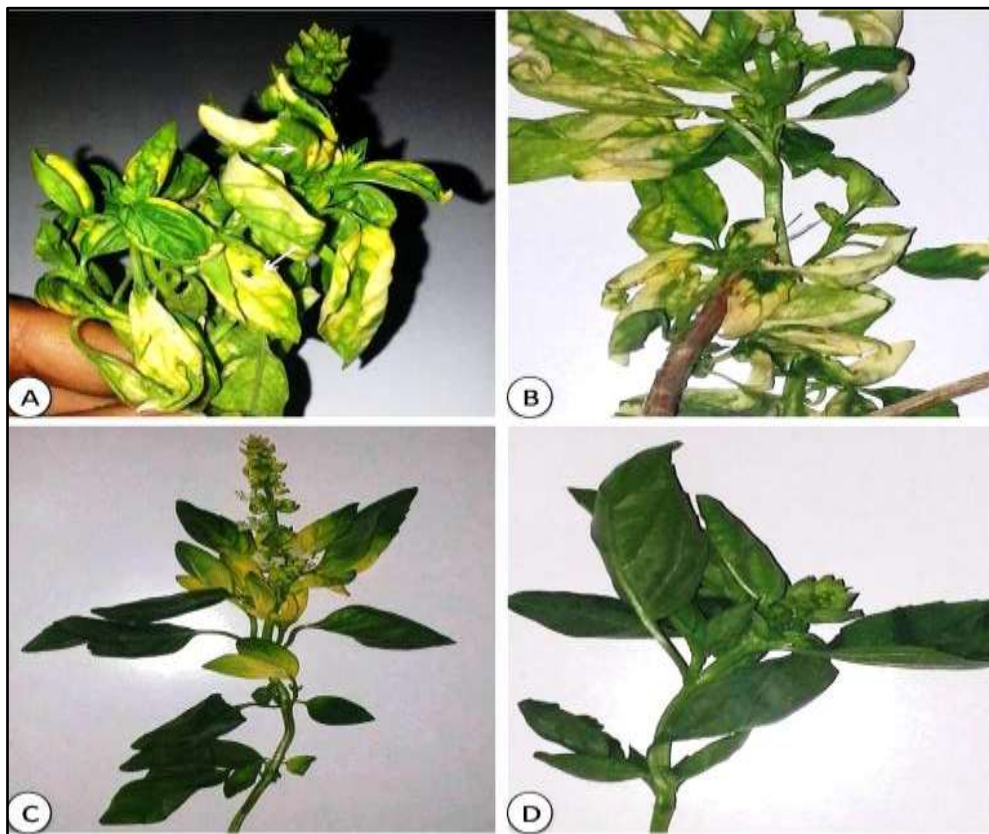


Fig. 1: Symptoms of naturally infected basil plants with *Alfalfa mosaic virus* (AMV). A: Folded leaves towards the main leaf vein, severe distortions and leaf necrosis (arrows). B: Warped leaves, severe mosaic white patches and leaf chlorosis. C: Severe bright yellow mosaic on emerging shoots and mature leaves. D: Healthy leaves of basil plant.

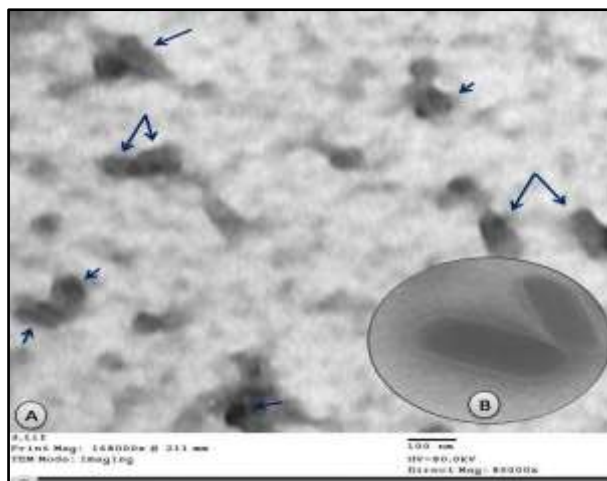


Fig. 2: Electron micrographs of negatively stained of *Alfalfa mosaic virus* particles. A: Electron micrograph of viral particles stained with 2% Phosphotungstic acid (PTA). Arrows point to a bacilliform particles. Scale bar is 100 nm, magnification 80000x. B: High magnification of area from a micrograph A stained with 2% PTA showing viral particles have a typical bacilliform structure with particles size of 112.5 nm in length and 57.5 nm in width. Scale bar is 100 nm, magnification 120000x.

Hence, leaf tissues from naturally infected basil plants showing yellow mosaic were used in mechanical inoculation experiments. At 7 days after inoculation, infection of *Chenopodium amaranticolor* and *C. quinoa* with *Alfalfa mosaic virus*, AMV, resulted in marked symptoms of chlorotic local lesions. The resulting local lesions on *C. quinoa* after three consecutive times were back inoculated onto *Nicotiana tabacum* var white burley. Inoculation on healthy basil seedlings, with inocula prepared from AMV-infected *N. tabacum*, resulted in marked symptoms of mild mosaic and yellow mosaic 14-22 days post inoculation, respectively similar to those on naturally infected plants. The symptoms shown by the other inoculated plants were reported in Table 2.

Table 1: Host reactions of healthy greenhouse-test plants to *Alfalfa mosaic virus* after mechanical transmission experiments.

Family	Recipient species ¹	AMV reaction symptoms ²
<i>Chenopodiaceae</i>	<i>Chenopodium amaranticolor</i>	CLL
	<i>Chenopodium quinoa</i>	CLL
<i>Fabaceae</i>	<i>Vicia faba</i>	MM
	<i>Phaseolus vulgaris</i>	LL
<i>Lamiaceae</i>	<i>Ocimum basilicum</i>	YM
	<i>Capsicum annuum</i>	LN
<i>Solanaceae</i>	<i>Datura stramonium</i>	SM
	<i>Nicotiana tabacum</i>	SM
	<i>Solanum tuberosum</i>	YM

¹ Species of plants arranged alphabetically by families.

² CLL: Chlorotic local lesions; LL: Local lesions; LN: Leaf necrosis; MM: mild mottle; SM: Systemic mosaic; YM: Yellow mosaic.

Molecular characterization of the AMV-CP

One step RT-PCR amplification of the AMV CP gene from infected basil leaves:

Electrophoresis analysis of the RT-PCR product showed specific bands at ~666 bp representing the expected size for the amplified AMV-CP gene, when total RNAs were efficiently extracted from naturally infected basil leaves as well as tested host species (*N. tabacum* and *O. basilicum*) (Fig.3, Lane1, 2 and 3). The primer pair,

designed on the basis of published sequences, successfully amplified AMV full length coat protein gene template in RT-PCR and confirmed the infection with AMV isolated from field-grown basil samples found in Egypt. No fragments were amplified from the RNA extracted from non-inoculated plants (Fig.3, Lane 4) or healthy control plants. RT-PCR was found to be highly efficient method of detection as shown in Figure 3.

Molecular cloning and Restriction analysis:

Following RT-PCR, the full length coat protein gene was successfully ligated into pCR[®]4-TOPO cloning vector and transformed in DH5 α cells. The selected clones containing the recombinant AMV-CP plasmid were digested using the *EcoRI* restriction enzyme. The electrophoresis analysis for the digested clones showed a clear band at the expected size of the AMV-CP gene (666bp) as well as a characteristic band at the size of the digested TOPO vector (4000 bp) as shown in Figure 4.

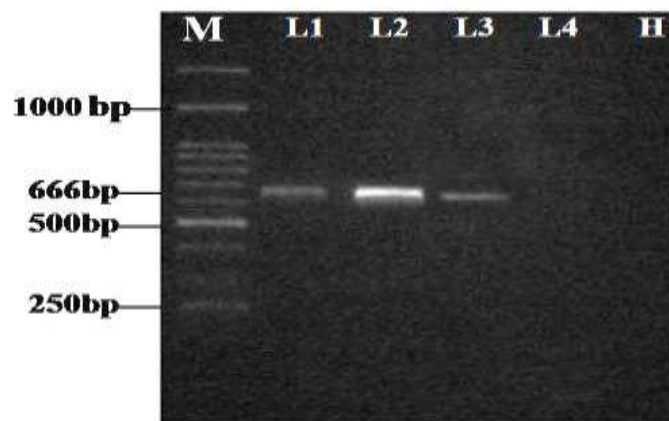


Fig. 3: Agarose gel electrophoresis patterns of RT-PCR products of *Alfalfa mosaic virus*. M: 1 kb DNA ladder. L1: Sample of the naturally infected basil leaves. L2: Sample of mechanically inoculated *Nicotiana tabacum* leaves. L3: Sample of mechanically inoculated *Ocimum basilicum* leaves. L4: Sample of non-inoculated *O. basilicum* leaves. H: Healthy control plant.

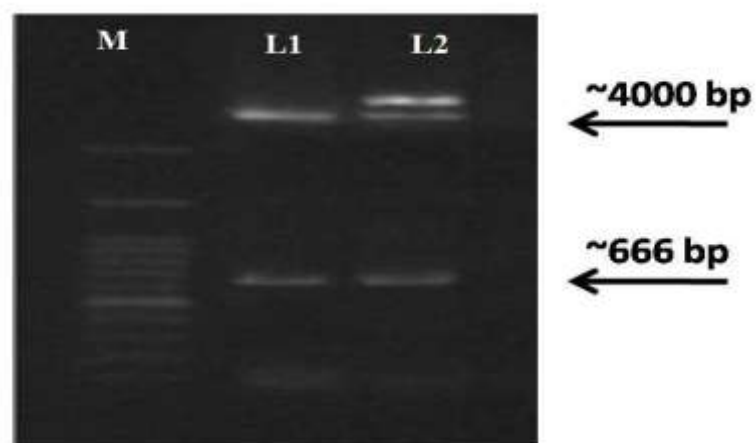


Fig. 4: Cloning efficiency through a ligation pCR[®]4-TOPO cloning vector. L1 and L2: Digestion of the plasmid using *EcoRI* showing the release of the AMV-CP gene at 666 bp and the digested TOPO vector at ~4000 bp. M: 1 kb molecular weight DNA ladder.

Sequencing of PCR products and phylogenetic analysis

The positive clones, whose fragments were correctly inserted, were selected for DNA sequencing. The nucleotide sequence of the coat protein (CP) gene of AMV isolated in Egypt was submitted to GenBank with accession number MH625710. The nucleotide sequence of CP gene was compared with those of 19 isolates from different geographical regions (Fig.5). The geographical origin and natural hosts for the isolates used in the phylogenetic analysis are illustrated in Table 2. A comparative analysis revealed that nucleotide sequence identity of CP gene among 20 isolates of AMV available in GenBank and AMV-isolate under study ranged from 91.30 to 96.40%. The highest degree of similarity (96.4%) was found with AMV-strain from Spain (HE591387, *Hibiscus rosa-sinensis*) showing bright yellow "aucuba"-type mosaic while the most distant isolate (91.3%) was reported from China (LK937168, *Nicotiana tabacum*). The sequence results also showed the high similarity (~94%) between AMV-Egypt isolate (MH625710) and two isolates from France (AJ130708, *Nicotiana glutinosa*) and Mexico (AY957607, *Leonotis nepetaefolia*). Additional comparisons showed that the Spanish isolate (HE591387, *Hibiscus rosa-sinensis*) has similarities (94.6 and 94.9%) to other two AMV-isolates from Egypt (HQ288892 and LN846979) isolated from potato and tomato, respectively (Fig.6).

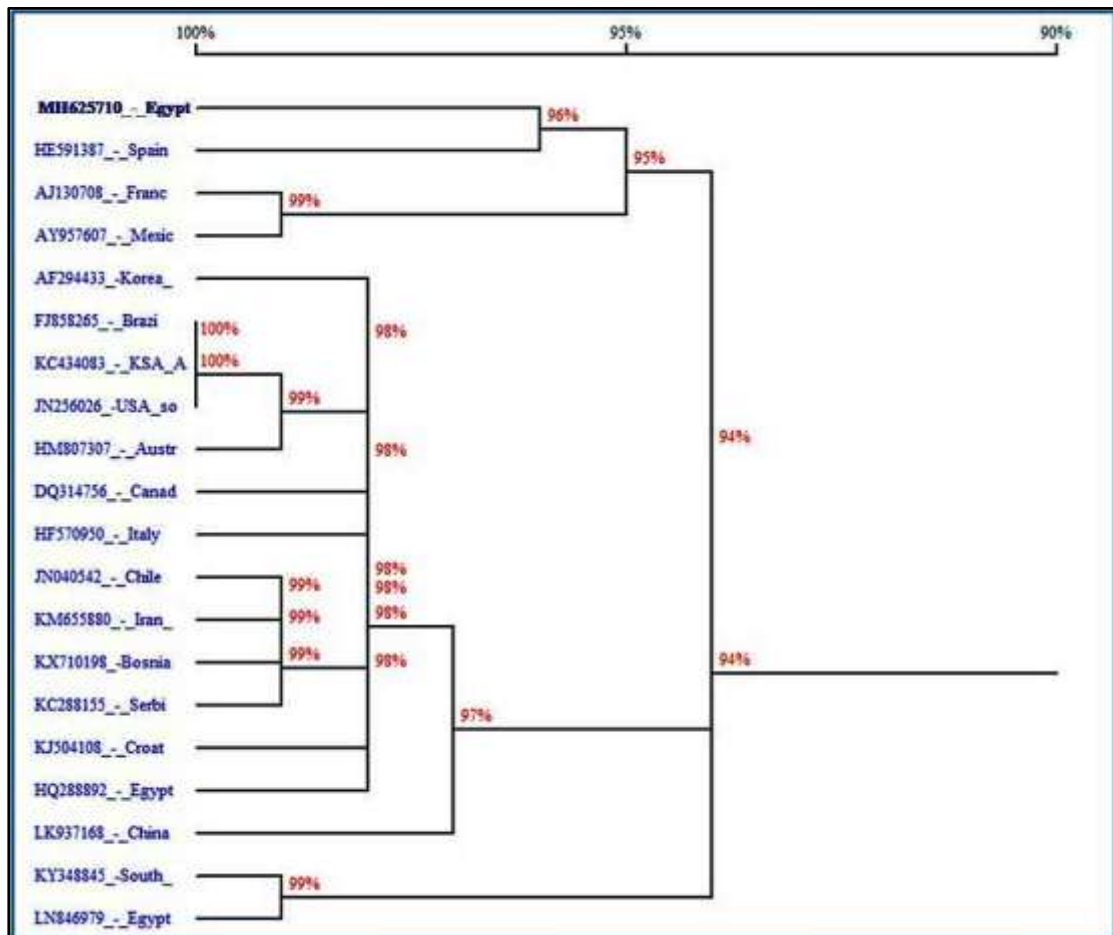


Fig. 5: Dendrogram depicting phylogenetic relationships among Egyptian isolate-MH625710 compared to other isolates available in databases.

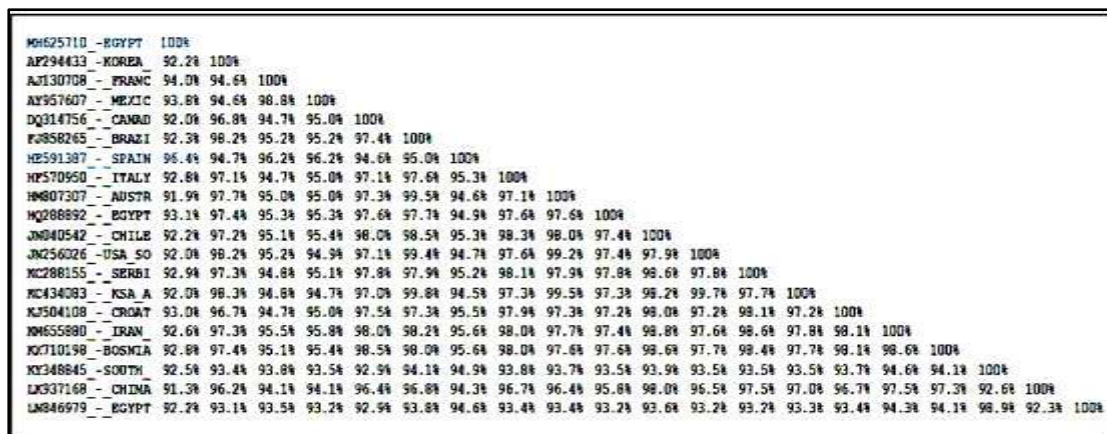


Fig. 6: The homology matrix for twenty sequences of AMV and relationships among themselves.

Effect of AMV-infection on the anatomical structure of basil leaves:

Light microscopy of cross sections through basil leaves stained with toluidine blue revealed distinctive histological differences between healthy and AMV-affected leaf cells. The mesophyll layer of the AMV-infected leaf lamina was disorganized and widely spaced; especially the palisade cells and the spongy mesophyll cells which were not at same size and shape (Fig. 7A) as compared with the fully organized layers in tissues of healthy leaf (Fig. 7B). Somewhat increase in the number of chloroplasts in the green parts (Fig. 8A) of symptomatic infected leaves as compared to yellow parts (Fig. 8B) of the same section. The deformations also extended to the vascular bundles area which contains the xylem and phloem parenchyma. The cross section illustrated that this area was disorganized and showed necrosis of the xylem tissue accompanied by disorganization of phloem parenchyma cells (Fig. 9A) while that of healthy tissue were fully organized without any necrosis of their units (Fig. 9B).

Table 2: Description of the accessions of AMV-isolates used in the phylogenetic analysis and the percentage of nucleotide sequence identity (%) of the Egyptian AMV-MH625710 isolated from basil.

	AMV-isolate Acc. Number.	Country	Host	Identity (%)*
1	AJ130708	FRANCE	<i>Nicotiana glutinosa</i>	94.00
2	AY957607	MEXICO	<i>Leonotis nepetaefolia</i>	93.80
3	DQ314756	CANADA	<i>Solanum tuberosum</i>	92.00
4	FJ858265	BRAZIL	<i>Medicago sativa</i>	92.30
5	HE591387	SPAIN	<i>Hibiscus rosa-sinensis</i>	96.40
6	HF570950	ITALY	<i>Araujia sericifera</i>	92.80
7	HM807307	AUSTRALIA	<i>Medicago sativa</i>	91.90
8	JN040542	CHILE	<i>Viburnum tinus</i>	92.20
9	JN256026	USA	<i>Glycine max</i>	92.00
10	KC288155	SERBIA	<i>Robinia pseudoacacia</i>	92.90
11	KC434083	KSA	<i>Medicago sativa</i>	92.00
12	KJ504108	CROATIA	<i>Lavandula X intermedia</i>	93.00
13	KM655880	IRAN	<i>Capsicum annum</i>	92.60
14	KX710198	BOSNIA	<i>Capsicum annum</i>	92.80
15	KY348845	S_KOREA	<i>Ligularia stenocephala</i>	92.50
16	AF294433	KOREA	<i>Solanum tuberosum</i>	92.20
17	LK937168	CHINA	<i>Nicotiana tabacum</i>	91.30
18	LN846979	EGYPT	<i>Lycopersicon esculentum</i>	92.20
19	HQ288892	EGYPT	<i>Solanum tuberosum</i>	93.10

^(a)Highest identity value is indicated in bold. All data from the <https://www.ncbi.nlm.nih.gov/nucleotide/> page.

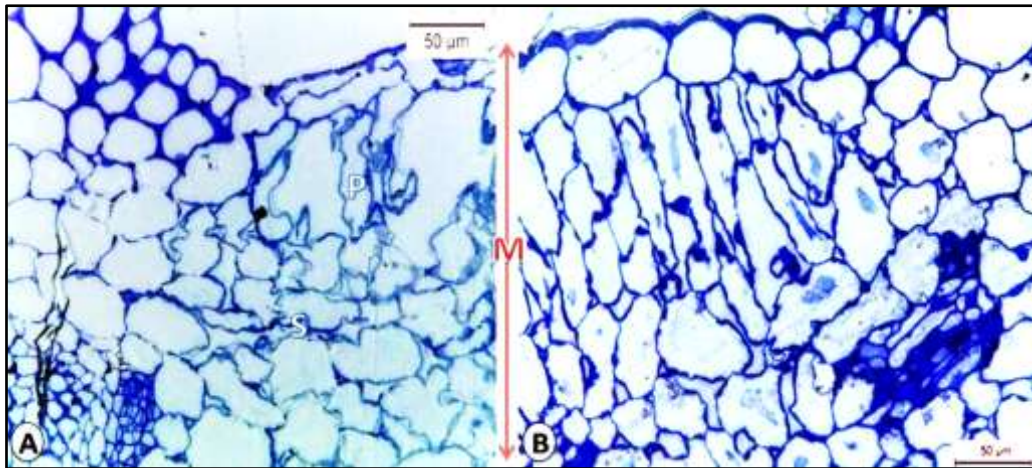


Fig. 7: Cross sections in basil leaf lamina. A: Section of AMV-infected leaf showing irregular palisade and spongy cells at mesophyll layer. B: Section of healthy leaf showing normal mesophyll layer with clear organization. Abbreviations: P: Palisade layer, S: Spongy layer, M: Mesophyll layer. x400

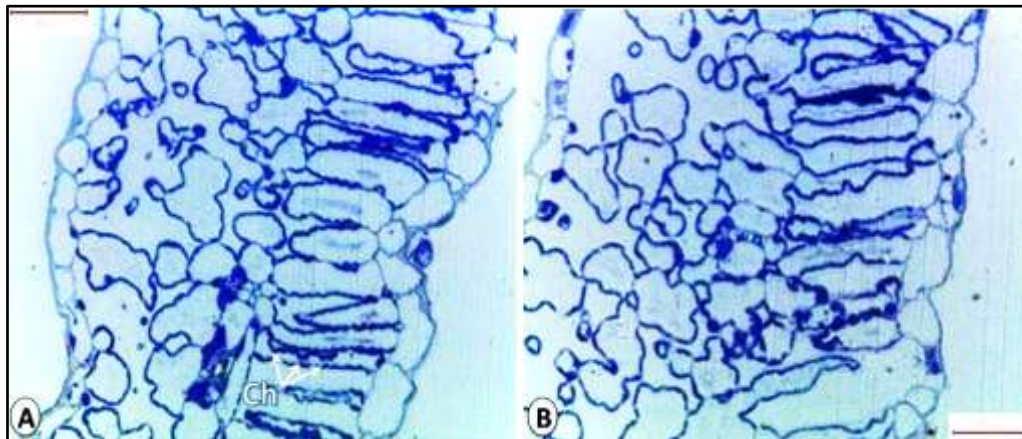


Fig. 8: Cross sections in palisade mesophyll cell infected with AMV. A: Cross section of green part of AMV-infected leaf showing increasing in the number of chloroplasts (Ch, arrows). B: Cross section of yellow part of the same AMV-infected leaf. x400

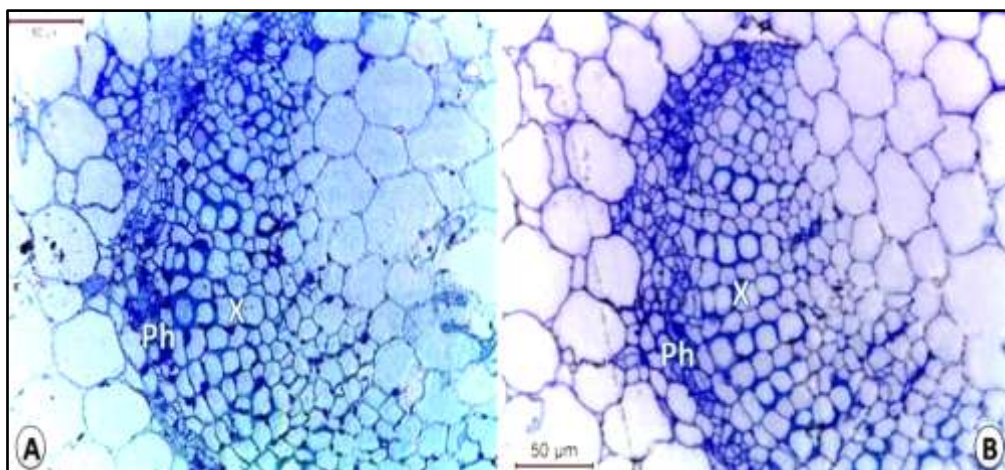


Fig. 9: Cross sections in vascular bundles. A: Section of AMV-infected basil leaf showing disorganization of the xylem (X) tissue and necrosis of the phloem (Ph). B: Section of healthy leaf showing normal vascular tissue without any necrosis of their units. x400

Ultrastructural effects of AMV infection:

Transmission electron microscopy of ultrathin sections of healthy and AMV-infected basil leaves was carried out. The results of ultrathin section visualization of infected tissue showed highly thickening of cell wall as well as dense and strongly adhered materials to the dilated cell wall which might be viroplasm, disruption of the nuclear membrane, the nucleus appeared a round ball-shaped and nucleolus disappeared in some cells (Fig. 10A) as compared with healthy cells (Fig. 10B).

Electron microscopy studies also revealed the accumulation of dense extracellular materials presumably around mitochondria in the phloem companion cells, enlargement of the nucleus which filled the cell cavity and contained a dark zone of dense materials or aggregates of virus particles randomly distributed in the cell. In some parts, the virus infection caused a mitochondrial degeneration (Fig. 11A). The cell wall was drastically affected exhibiting unusual thickening (Fig. 11B). The plasmodesmata showed several degrees of dilation to facilitate existing virus particles movement. The necrotized cytoplasm was characterized by multiple vacuoles which some of them contained virus like particles (Fig. 11B).

In the green parts of the AMV-infected leaf lamina, AMV-infection established the accumulation of intracellular viral particles; extended from chloroplast outwardly to the cell wall (Fig. 12A). In the yellow parts of the AMV-infected leaf lamina; Figure 12B demonstrates the existence of AMV-virus particles distributed along the chloroplast and at the membrane that surrounds the vacuole (tonoplast). The observed viral assemblies were always associated with extensively degraded cell wall. Chloroplast in the yellow parts is irregular in their shape with different structures such as membrane expansion toward the cell wall followed by membrane retraction causing cytoplasmic cavity and broken of outer envelope membrane. Profound changes in the chloroplast were observed, e.g., large vacuole and complete destruction in grana and thylakoids. On the other side, the chloroplasts in the green parts were not drastically affected. Meanwhile, the cell wall was irregular in shape (Fig. 12A) as compared to that of healthy tissue sample (Fig. 12C).

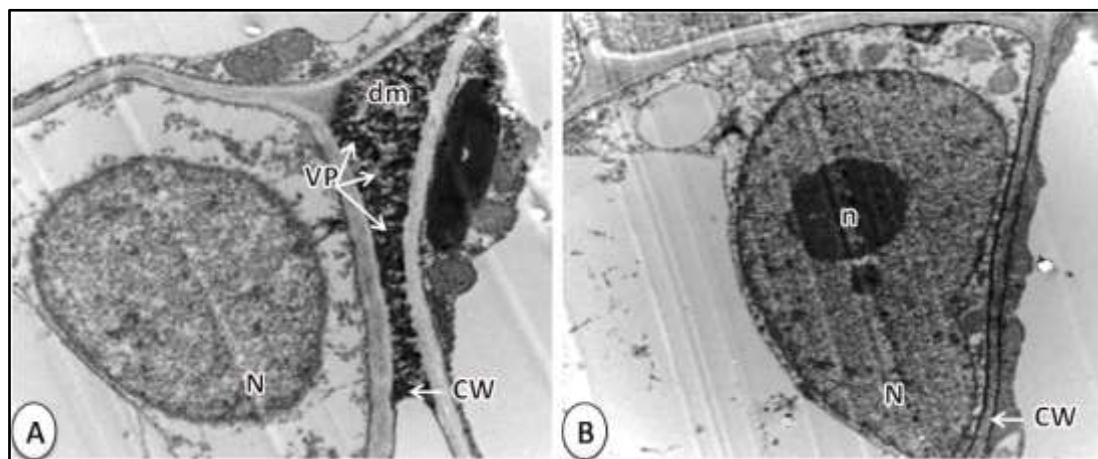


Fig. 10: Electron micrographs of ultrathin sections of basil leaf tissues. A: An electron micrograph of AMV-infected leaf tissue displays the disorders of nucleus (N), absence of the nucleolus (n), visible particles of AMV (VP, arrows) or deposited materials (dm) which affects the cell wall (CW) structure (12000x). B: An electron micrograph of healthy leaf tissue showing normal thickness of cell wall (CW) and spherical structure of nucleolus (n) within the nucleus (N) of the cell (10000x). The bars indicate 500 nm.

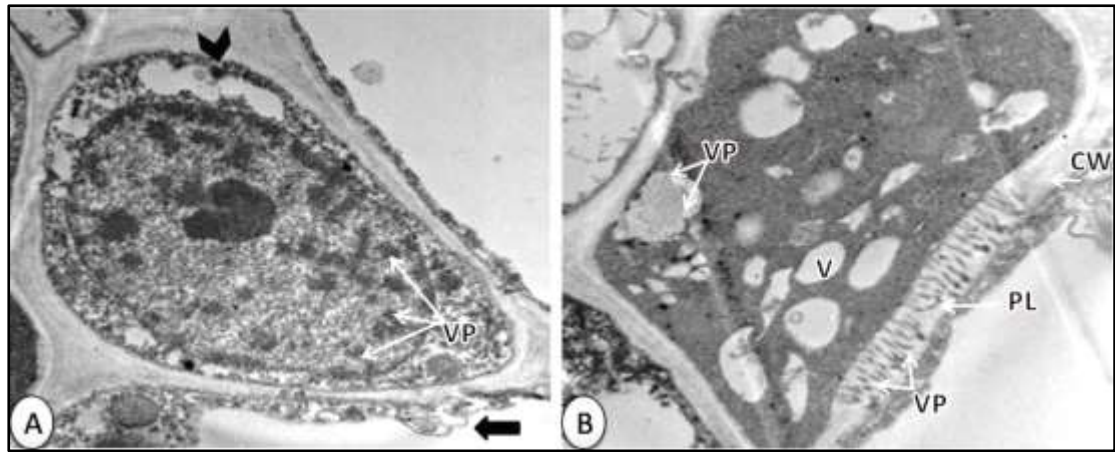


Fig. 11: Electron micrographs of ultrathin sections of phloem tissues of AMV-infected basil. A: An electron micrograph showing several virus particles (VP, arrows) per companion cell associated with irregular nuclear shape. The black arrow indicates irregular dense extracellular materials associated with masked mitochondrion. The black arrowhead indicates degeneration of mitochondria inside the cell (12000x). B: An electron micrograph of phloem parenchyma cell showing thickened cell wall (CW), virus particles (VP, arrows) in deformed plasmodesmata (PL), many abnormal vacuoles (V), necrosis of cytoplasm (15000x). The bars indicate 500 nm.

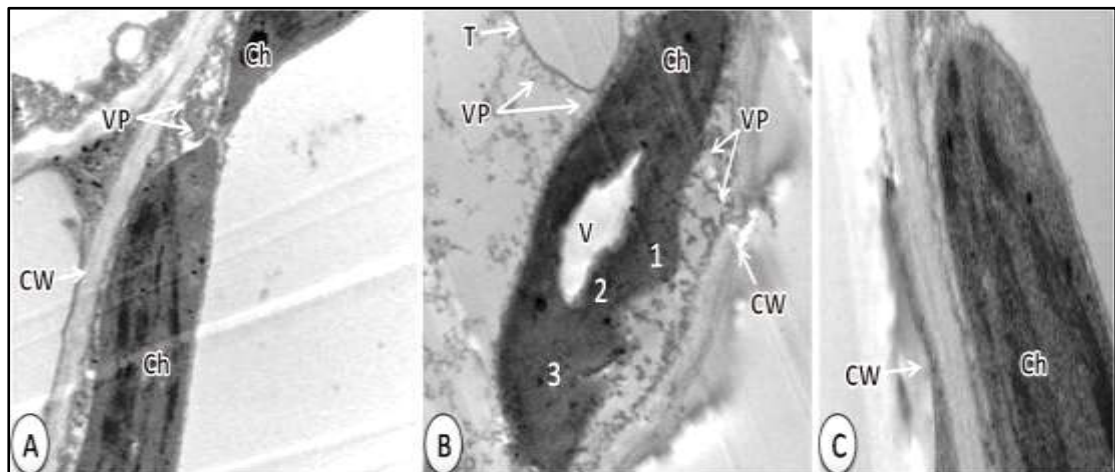


Fig. 12: Electron micrographs of ultrathin sections of chloroplasts (Ch) of basil-tissues. A: An electron micrograph of the green parts of the AMV-infected leaf lamina displays the accumulations of viral particles (VP, arrows) between the irregular cell wall (CW) and the chloroplast membrane (15000x). B: An electron micrograph of the yellow parts of the AMV-infected leaf lamina displays complete destruction of grana and thylakoids, the degradation of cell wall (CW) and the distribution of viral particles (VP, arrows) around the tonoplast (T) and the chloroplast membrane. Chloroplast has a central large vacuole (V) and irregular membrane structures such as ⁽¹⁾ membrane extrusions, ⁽²⁾ viral particles-bound cytoplasmic cavity, and ⁽³⁾ broken envelope membrane (20000x). C: An electron micrograph of healthy leaf lamina showing normal chloroplast (CL) and cell wall (30000x). The bars indicate 500 nm.

DISCUSSION

Until this study *Alfalfa mosaic virus* (AMV) has not been characterized at the molecular level as well as cytological changes accompanied with the viral infection

despite previously serological evidences of presence of AMV in basil plants in Egypt (Shafie *et al.*, 1997). Therefore, the causal agent of viral disease has been isolated from one of the active regions of the country (Beni Suef governorate) for producing basil, and primarily identified on the basis of symptom expression and morphological properties along with serological and molecular tests.

The ease and rapid with which the virus identification was performed (within 10 minutes) after a simple negative stain preparation, indicate that electron microscopy is one of the most useful tools in diagnosis as well as direct virus particle observation (Gelderblom and Hazelton, 2000; Otulak *et al.*, 2014). In the present study, electron microscopy revealed AMV-particles were bacilliform shaped, have lengths 112.5 nm with 57.5 nm in width (Hull, 1969; Luque and Reguera, 2013; Abdalla *et al.*, 2016).

Alfalfa mosaic virus is a wide spread, common virus infecting a variety of plants and consisting of many strains that differ in symptomatology on various hosts (Hull, 1969). In the present study, calico symptoms, which consist of a bright yellow and green aucuba mosaic, of diseased basil leaves were characteristic of AMV. Several reports have described the natural occurrence of AMV of calico mosaic type on Parsley (Campbell and Melugin, 1971), Soybean (Almeida *et al.*, 1982), Potato (Xu and Nie, 2006) and *Tecoma capensis* (Parrella *et al.*, 2011). Subsequently, a new AMV-strain was reported infecting *Hibiscus rosa-sinensis* in Spain (Parrella *et al.*, 2012) which showed the bright yellow "aucuba"-type mosaic. The obtained data revealed that nucleotide sequences of the AMV isolate from Spain and the Egyptian isolate under study were similar to each other, with 96.4% homology.

It is important to state that the Spanish isolate was also closely related to the other two AMV-isolates from Egypt, with greater than 94.5% nucleotide identity, which obtained from diseased potato and tomato plants (HQ288892, LN846979, respectively). Moreover, phylogenetic analyses of sequences of AMV-CP showed a high level of diversity (3.6-8.7%) among the twenty AMV-isolates from different parts of the world. So, a molecular characterization of viral coat protein sequences did not confirm a 100 percent correlation between the origin of viral isolate or host range. Taking into account, the spreading efficiency of AMV by mechanical inoculation caused local lesions or systemic symptoms in the nine species of different families, exactly similar to those presented by Lee *et al.* (1985), Zitikaite and Samuitiene (2008), Sabry *et al.* (2010), Stankovic *et al.* (2014) and Abdalla *et al.* (2016). Such wide diversity confirms only the great ability of the virus to overcome the natural defense responses in a wide group of plant hosts more than 400 host (Parrella *et al.*, 2000; Sabry *et al.*, 2010), with confirmation of the fact that AMV is infectious only in the presence of the viral coat protein (CP), that plays a main role in the viral life cycle (Bol *et al.*, 1971; Balasubramaniam *et al.*, 2014). Where, the data presented in this study revealed that the gene derived from coat protein (AMV-CP) required for viral spread, was detected by a clear band corresponding to the expected size of the amplification products of approximately 666 base pairs, as consistent with previous findings by Xu and Nie (2006), El-Helaly *et al.* (2012) and AL-Saleh and Amer (2013).

Based on the current study, several evidences point towards the presence of dark zones associated with electron-dense bodies in intracellular compartments of various cell types, of which AMV-particles and other deposited materials relevant for viroplasm, that associated with cytoplasm in the infected phloem cells, nucleus of companion cell, plasmodesmata, chloroplast and the membrane that surrounds the central vacuole of the plant.

Accumulating evidence demonstrates that virus interacts with the host cytoskeleton and may be used different membranes for its movement or its encoded proteins resulted in a number of the observed severe changes on the cellular level. This would be in agreement with the findings of Gerola *et al.* (1969), who described the appearance of AMV-particles in the infected yellow leaf tissues of basil plant and fill large areas of the cytoplasm, contain a number of vacuoles of various sizes as well as marked alterations of the chloroplasts and disappearance of grana and thylakoids. Also, according to Gerola *et al.* (1969) the appearance of large vacuole inside the chloroplast as well as the frequent formation of large vacuoles inside the cytoplasm might also be due to osmotic imbalance brought about by the virus infection. Likewise, Favali and Conti (1970) observed accumulation of viral particles in chloroplasts of basil plants infected with AMV. This is also consistent with what was published in this regard, the association of AMV replication with different membranes of infected cells, including the cytoplasm, nucleus, nucleolus, vacuole, chloroplast and tonoplast (Vanpeltheerschap *et al.*, 1987; Sanfacon, 2005; Ibrahim *et al.*, 2012). Also, the localization of AMV-viral particles in plasmodesmata is consistent with the observation that the plasmodesmata connecting sieve elements to companion cells are structurally distinctive (have a large size) from other plasmodesmata between other cells (Leisner and Turgeon, 1993; Van Bel and Kempers, 1997). It is to be noted that, viroplasm structures in cells infected with plant viruses are generally sites of virus replication, virion assembly and in some cases are involved in cell-to-cell movement (Qiao *et al.*, 2017).

Generally, nucleolus and chloroplast targeting appears to be a general feature of several plant viruses, like as *Potato leaf roll virus*, *Prune dwarf virus* and *Tomato ring spot nepovirus* (Haupt *et al.*, 2005; Hamed *et al.*, 2012; El-Banna *et al.*, 2014). However, recent microscopic study showed that changes due to AMV infection in cell membranes or viral movement from cell to cell apparently similar to *Prune dwarf virus* (Koziel *et al.*, 2018).

So, external symptoms, displayed by AMV-infected basil plants, were strictly correlated with the histological and ultrastructural changes occurring inside cells. For instance: bright yellow mosaic, severe mosaic, necrosis and chlorosis. The previous symptoms were accompanied by a degradation of mesophyll layers, outer structural change of chloroplast, decreasing in the number chloroplasts and the destruction of the intracellular subunits (grana and thylakoids).

CONCLUSION

The presented findings show more support for the first report (Shafie *et al.*, 1997) of natural occurrence of *Alfalfa mosaic virus* on basil plants in Egypt but to our knowledge, this is the first molecular identification of AMV on basil plants in Egypt (Accession no. MH625710). The presented findings reflect the morphological symptoms displayed by basil plants as a result of the histological symptoms induced by *Alfalfa mosaic virus*. Despite rapid and accurate advances in diagnostic technologies, diagnostic electron microscopy could be also used as another tool for identifying viral infection.

AUTHOR DETAILS

¹Virus and Phytoplasma Research Department, Plant Pathology Research Institute, Agricultural Research Center ARC, Giza 12619, Egypt.

²Plant Pathology Department, Faculty of Agriculture, Cairo University, Giza 12613, Egypt.

RECEIVED: Oct. 2018; **ACCEPTED:** Dec. 2018; **PUBLISHED:** Jan. 2019

REFERENCES

- Abdalla, O.A.; Eraky, Amal I.; Mohamed, Safynaz A. and Fahmy, F.G. (2016):** Molecular identification of viruses responsible for severe symptoms on potato (*Solanum* sp.) growing in Assiut Governorate (Upper Egypt). *Int. J. Virol. Stud. Res.*, 4(3):29-33.
- Almeida, A.M.; Bianchini, A.; Costa, A.S. and Vega, J. (1982):** Calico mosaic, a new virus disease of soybean in Brazil. *J. Fitopatol. Bras.*, 7(1):133-138.
- AL-Saleh, M.A. and Amer, M.A. (2013):** Biological and molecular variability of *Alfalfa mosaic virus* affecting alfalfa crop in Riyadh region. *Plant Pathol. J.*, 29(4):410-417.
- Ammara, Um E.; Al-Ansari, M.; Al-Shihi, A.; Amin, I.; Mansoor, Sh.; Al-Maskari, A.Y. and Al-Sadi, A.M. (2015):** Association of three *begomoviruses* and a beta-satellite with leaf curl disease of basil in Oman. *Can. J. Plant Pathol.*, 37:506-513.
- Ausubel, F.M.; Brent, R.; Kingston, R.E.; Moore, D.D.; Seidman, J.G.; Smith, J.A. and Struhl, K. (1989):** Current protocols in molecular biology. John Wiley and Sons, New York.
- Balasubramaniam, M.; Kim, B.S.; Hutchens-Williams, H.M. and Loesch-Fries, L.S. (2014):** The photosystem II oxygen-evolving complex protein PsbP interacts with the coat protein of *Alfalfa mosaic virus* and inhibits virus replication. *Mol. Plant Microbe Interact.*, 27:1107-1118.
- Bol, J.F.; Van Vloten-Doting, L. and Jaspars, E.M. (1971):** A functional equivalence of top component a RNA and coat protein in the initiation of infection by *Alfalfa mosaic virus*. *Virol.*, 46:73-85.
- Campbell, R.N. and Melugin, S.A. (1971):** *Alfalfa mosaic virus* strains from carrot and parsley. *Plant Dis. Rep.*, 55(4):322-325.
- Clark, M.F. and Adams, A.N. (1977):** Characteristics of the microplate method of enzyme linked immunosorbent assay for the detection of plant viruses. *J. Gen. Virol.*, 34:475-483.
- Davino, S.; Accotto, G.P.; Masenga, V.; Torta, L. and Davino, M. (2009):** Basil (*Ocimum basilicum*), a new host of *Pepino mosaic virus*. *Plant Pathol.*, 58:407.
- El-Banna, Om-Hashem M.; Awad, M.A.E.; Abbas, M.S.; Waziri, Hoda M.A. and Darwish, Huda S.A. (2014):** Anatomical and ultrastructural changes in tomato and grapevine leaf tissues infected with *Tomato ringspot nepovirus*. *Egyptian J. Virol.*, 11(2):102-111.
- El-Helaly, H.S.; Ahmed, A.A.; Awad, M.A. and Soliman, A.M. (2012):** Biological and molecular characterization of potato infecting *Alfalfa mosaic virus* in Egypt. *Inter. J. Virol.*, 8:106-113.
- FAO/WHO (2017):** Food and Agriculture Organization of the United Nations/World Health Organization. Food Standards Programme. Report of the 3rd Session of the codex committee on spices and culinary herbs, Appendix VIII-Proposal for new work on a codex standards for Basil, pp 57.
- Favali, M.A. and Conti, G.G. (1970):** Ultrastructural observations on the chloroplasts of basil plants either infected with different viruses or treated with 3-amino-1,2,4-triazole. *Protoplasma*, 70:153-166.
- Gelderblom, H.R. and Hazelton, P.R. (2000):** Specimen collection for electron microscopy. *Emerg. Infect. Dis.*, 6(4):433-434.
- Gerola, F.M.; Bassi, M. and Betto, E. (1969):** A Submicroscopical study of leaves of Alfalfa, Basil, and Tobacco experimentally infected with *Lucerne mosaic virus*. *Protoplasma*, 67:307-318.

- Hamed, A.H.; El-Banna, Om-Hashem M.; Ghanem, G.A.M.; Elnagaar, H. and Shafie, M.S. (2012):** Isolation and identification of *Tobacco rattle tobnavirus* affecting Onion (*Allium cepa* L.) Plants in Egypt. *Int. J. Virol.*, 8:39-49.
- Haupt, S.; Stroganova, T.; Ryabov, E.; Kim, S.H.; Fraser, G.; Duncan, G.; Mayo, M.A.; Barker, H. and Taliansky, M. (2005):** Nucleolar localization of *Potato leaf roll virus* capsid proteins. *J. Gen. Virol.*, 86:2891-2896.
- Holcomb, G.E.; Valverde, R.A.; Sim, J. and Nuss, J. (1999):** First report on natural occurrence of *Tomato spotted wilt tospovirus* in basil (*Ocimum basilicum*). *Plant Dis.*, 83(10):966.
- Hull, R. (1969):** *Alfalfa mosaic virus*. *Adv. Virus Res.*, 15:365-433.
- Ibrahim, A.; Hutchens, H.M.; Berg, R.H. and Loesch-Fries, S. (2012):** *Alfalfa mosaic virus* replicase proteins, P1 and P2, localize to the tonoplast in the presence of virus RNA. *Virol.*, 433:449-461.
- Kahn, R.P. and Monroe, R.I. (1963):** Detection of tobacco vein necrosis (strain of *potato virus Y*) in *Solanum carensaii* and *S. andigenum* introduced into the United States. *Phytopathol.*, 53:1356-1359.
- Koziel, E.; Otulak-Koziel, K. and Bujarski, J.J. (2018):** Ultrastructural analysis of *Prune dwarf virus* intercellular transport and pathogenesis. *Int. J. Mol. Sci.*, 19(9):2570.
- Kumlachew, A. (2015):** Detection of diseases, identification and diversity of viruses: A review. *J. Biol., Agric. Healthcare*, 5(1): 204-213.
- Lee, S.H.; Choi, Y.M.; Kim, J.S. and Chung, B.J. (1985):** Identification of *Alfalfa mosaic virus* from soybean. *Kor. J. Plant Pathol.*, 1:33-37.
- Leisner, S.M. and Turgeon, R. (1993):** Movement of virus and photoassimilate in the phloem: A comparative analysis. *Bioessays*, 15:741-748.
- Luque, A. and Reguera, D. (2013):** Theoretical studies on assembly, physical stability and dynamics of viruses. *Subcell Biochem.*, 68:553-595.
- Noordam, D. (1973):** Identification of plant viruses: Methods and experiments. Centre for Agricultural Publishing and Documentation, Wageningen, Netherlands. 207pp.
- Otulak, K.; Koziel, E. and Garbaczewska, G. (2014):** Seeing is believing. The use of light, fluorescent and transmission electron microscopy in the observation of pathological changes during different plant-Virus interactions. In *Microscopy: Advances in Scientific Research and Education*, 6th ed.; Mendez-Vilas, A., Ed.; Formatex Research Center: Badajoz, Spain, Volume 1, pp. 367-376.
- Parrella, G.; Acanfora, N.; Orilio, A.F. and Navas-Castillo, J. (2011):** Complete nucleotide sequence of a Spanish isolate of *Alfalfa mosaic virus*: Evidence for additional genetic variability. *Arch. Virol.*, 156:1049-1052.
- Parrella, G.; Fiallo-Olive, E. and Navas-Castillo, J. (2012):** First report of China Rose (*Hibiscus rosa sinensis*) as a host of *Alfalfa mosaic virus* in Spain. *Plant Dis.*, 96(3):462-462.
- Parrella, G.; Lanave, C.; Marchoux, G.; Finetti-Sialer, M.M.; Di Franco, A. and Gallitelli, D. (2000):** Evidence for two distinct subgroups of *Alfalfa mosaic virus* AMV from France and Italy and their relationship with other AMV strains. *Archive of Virology*, 145(12):2659-2667.
- Poojari, S. and Naidu, R.A. (2013):** First report of *Impatiens necrotic spot virus* (INSV) infecting basil (*Ocimum basilicum*) in the United States. *Plant Dis.*, 97(6):850-851.
- Qiao, W.; Medina, V. and Falk, B.W. (2017):** Inspirations on virus replication and cell-to-cell movement from studies examining the cytopathology induced by *Lettuce infectious yellows virus* in plant cells. *Front. Plant Sci.*, 8:1672.

- Rocchetta, I.; Leonard, P.I. and Filho, G.M.A. (2007):** Ultrastructure and X-ray microanalysis of *Euglena gracilis* (Euglenophyta) under chromium stress. *Phycologia*, 46:300-306.
- Sabry, Y.M.; Abdel-Sabour, G.A. and Karel, P. (2010):** Differentiation study between *Alfalfa Mosaic Virus* and *Red Clover Mottle Virus* affecting broad bean by biological and molecular characterization. *Int. J. Virol.*, 6:224-239.
- Sanfacon, H. (2005):** Replication of positive-strand RNA viruses in plants: Contact points between plant and virus components. *Can. J. Bot.*, 83:1529-1549.
- Sanz, N.T.; Chen, T.H. and Lai, P.Y. (2001):** A newly discovered mosaic disease of bush basil (*Ocimum basilicum*) in Taiwan. *Plant Pathol. Bulletin*, 10:155-164.
- Shafie, M.S.A.; Zaher, Nahed A.; El-Kady, M.A.S. and Abu-Zeid, A.A. (1997):** Natural occurrence of *Alfalfa mosaic virus* on Basil plants in Egypt. *J. Appl. Sci.*, 12:15-30.
- Sinha, S. and Samad, A. (2019):** First report of *Cucumber mosaic virus* associated with yellowing mosaic disease of African basil (*Ocimum gratissimum*) in India. *Plant Dis.*, 103(1):167.
- Stankovic, I.; Vrandecic, K.; Cosic, J.; Milojevic, K.; Bulajic, A. and Branka, K. (2014):** The spreading of *Alfalfa mosaic virus* in lavandin in Croatia. *Pestic. Phytomed. (Belgrade)*, 29(2):115-122.
- Van Bel, A.J.E. and Kempers, R. (1997):** The pore/plasmodesm unit: Key element in the interplay between sieve element and companion cell. *Prog. Bot.*, 58:277-291.
- Vanpeltheersch, H.; Verbeek, H.; Slot, J.W. and Vanvlotendoting, L. (1987):** The location of coat protein and viral RNAs of *Alfalfa mosaic virus* in infected tobacco leaves and protoplasts. *Virol.*, 160:297-300.
- Wintermantel, W.M. and Natwick, E.T. (2012):** First report of *Alfalfa mosaic virus* infecting basil (*Ocimum basilicum*) in California. *Plant Dis.*, 96(2):295.
- Xu, H. and Nie, J. (2006):** Identification, characterization and molecular detection of *Alfalfa mosaic virus* in Potato. *Virol.*, 96 (11):1237-1242.
- Zitikaite, I. and Samuitiene, M. (2008):** Identification and some properties of *Alfalfa mosaic alfamovirus* isolated from naturally infected tomato crop. *Biologija*, 54(2):83-88.

Cite this article as:

El-Attar *et al.*, (2019): Molecular Characterization of *Alfalfa Mosaic Virus* and Its Effect on Basil (*Ocimum basilicum*) Tissues in Egypt. *Journal of Virological Sciences*, Vol.5: 97- 113.